9248 *Macromolecules* **2010**, *43*, 9248–9256
DOI: 10.1021/ma101925x

Macromolecules
ARTICLE

Trimethylenedipyridinium Dendrimers: Synthesis and Sequential Complexation of Anthraquinone Disulfonate in Molecular Shells

Murugavel Kathiresan and Lorenz Walder*

Institute of Chemistry OCII, University of Osnabrueck, Barbarastrasse 7, Osnabrueck, D 49069, Germany

Received August 20, 2010; Revised Manuscript Received September 28, 2010

ABSTRACT: The synthesis of a new class of polycationic dendrimers of generation 0, 1, and 2 ($\mathbf{G_0}$ (1.07 nm), $\mathbf{G_1}$ (1.63 nm), and $\mathbf{G_2}$ (3.03 nm)) is described. Core and 2-fold branching units consist of interconnected 1,3,5-tris(methylene)benzene and 4,4′-trimethylenedipyridinium units. 4-*tert*-Butylbenzyl has been used as the peripheral end group because best solubility of the dendrimers was achieved. The dendrimers act as a host for anthraquinone-2,6-disulfonate (AQDS) and can be stoichiometrically titrated and even overcharged as shown by ^{1}H NMR, DOSY and cyclic voltammetry. Upon loading them with AQDS, the dendrimers undergo first a contraction, they reach a minimum hydrodynamic radius for complete charge compensation and they reopen when overcharging takes place. The contraction is supported by MM+ calculations. Upon stepwise loading of $\mathbf{G_2}$ (42 positive charges) with AQDS (2 negative charges), the first 3 mol equiv (6 negative charges) occupy the innermost dendrimer shell (consisting of 6 positive charges), the next 6 equiv (12 negative charges) occupy the middle shell (12 positive charges), and the last 12 equiv AQDS (24 negative charges) occupy the outermost shell of the dendrimer (24 positive charges), as supported by ^{1}H NMR titrations yielding the magic equivalent numbers of 3, 9 = 3 + 6, and 21 = 3 + 6 + 12.

1. Introduction

Dendrimers belong to a unique class of synthetic polymers with well-defined, highly branched architecture emanating from a central core through a stepwise, repetitive reaction sequence. Since the pioneering work of Vögtle,[1] Tomalia,[2] Newkome,[3] and Frechet,[4] the synthesis,[5] a special emphasis on functionalization,[6] and the tuning of their properties became a central point of the research. The microenvironments in the interior and at the periphery of the dendrimers cannot be overestimated in many applications.[7] The empty space can be occupied by molecular guests with the dendrimer playing the role of the host.[8] The guest molecules can be complexed at the dendrimer periphery or in void regions within the dendrimer. Thus, the encapsulation of guest molecules into dendritic cavities[8d,9] is of prominent importance. Often the take-up of guest molecules is accompanied by conformational changes of the dendrimer as a consequence of the supramolecular complex formation. However, conformational changes are also known to occur upon contact with pure solvents or upon acid base reactions of dissociable groups within or at the periphery of a dendrimer.[5e,10]

Typical methods for the study of host−guest interactions involve the following: (i) ^{1}H NMR techniques (interaction accompanied by a change in chemical shift); (ii) DOSY (diffusion-ordered spectroscopy) (interaction accompanied by a change of the diffusion coefficient of host or guest);[9a,11] (iii) cyclic voltammetry (interaction accompanied by a shift in electrochemical potential of an electroactive host or guest).[12,13] Other methods such as UV−vis, Raman spectroscopy, Maldi−TOF, and fluorescence titrations have also been used to probe the host−guest interactions.[14]

We have reported earlier on a similar series of dendrimers and oligomers consisting of 4,4′-bipyridinium subunits instead of 4,4′-trimethylenedipyridinium with focus on the synthesis, the generation dependent CT complexation, the molecular diode behavior, and their electrochromic properties.[15] Their host−guest chemistry was exploited by Balzani et al.[14d,16] It has further been shown that the viologen dendrimers have antiviral properties and that a series of related viologen dendrimers behave as gene-transfecting agents.[17] Typically, such applications rely on the viologen dendrimer's ability to wrap onto large biological structures. We consider their practical use in medicine as questionable because of the inherent toxicity of the viologen monomer, related to its low reduction potential.[18] Principally most cationic polyelectrolytes (a prerequisite for gene transfection/DNA condensation) can interact nonspecifically with other cellular compounds leading ultimately to cell death, a side reaction that can be partially controlled by the dendrimers peripheral groups and its generation.[19] Cationic nonelectroactive dendrimers based on 4,4′-trimethylenedipyridinium subunits might show less toxicity and better conformational adaptability because of the trimethylene function disrupting the π-resonance and displaying higher flexibility.

Herein we report on the synthesis of a new class of cationic dendrimers based on benzylic trimethylenedipyridinium subunits. As worked out above, this modification renders the dendrimer less electroactive (less toxic) and more flexible (more adaptive). Their medicinal value will therefore be studied in the near future. In the current article we report on the synthesis and on fundamental complexation studies of organic anions within the voids of the cationic dendrimers.

A few years ago K. Yamamoto and co-workers have reported on the sequential complexation of guest molecules (inorganic Lewis acids) by phenylazomethine dendrimers with the imine functionalities acting as Lewis base coordination sites.[14f,20] The authors have shown by UV/vis titration that the guest molecules fill the dendrimer radially stepwise starting with the innermost shell. There is no report on other dendrimer/guest combinations showing the same stepwise charging mode, and the question is still not solved, if the phenomenon observed by Yamamoto is

*Corresponding author. E-mail: Lowalder@uos.de.

 Published on Web 10/19/2010

Scheme 1. Synthesis of Core, Branching, and Peripheral Units for the Divergent and Convergent Dendrimer Synthesis[a]

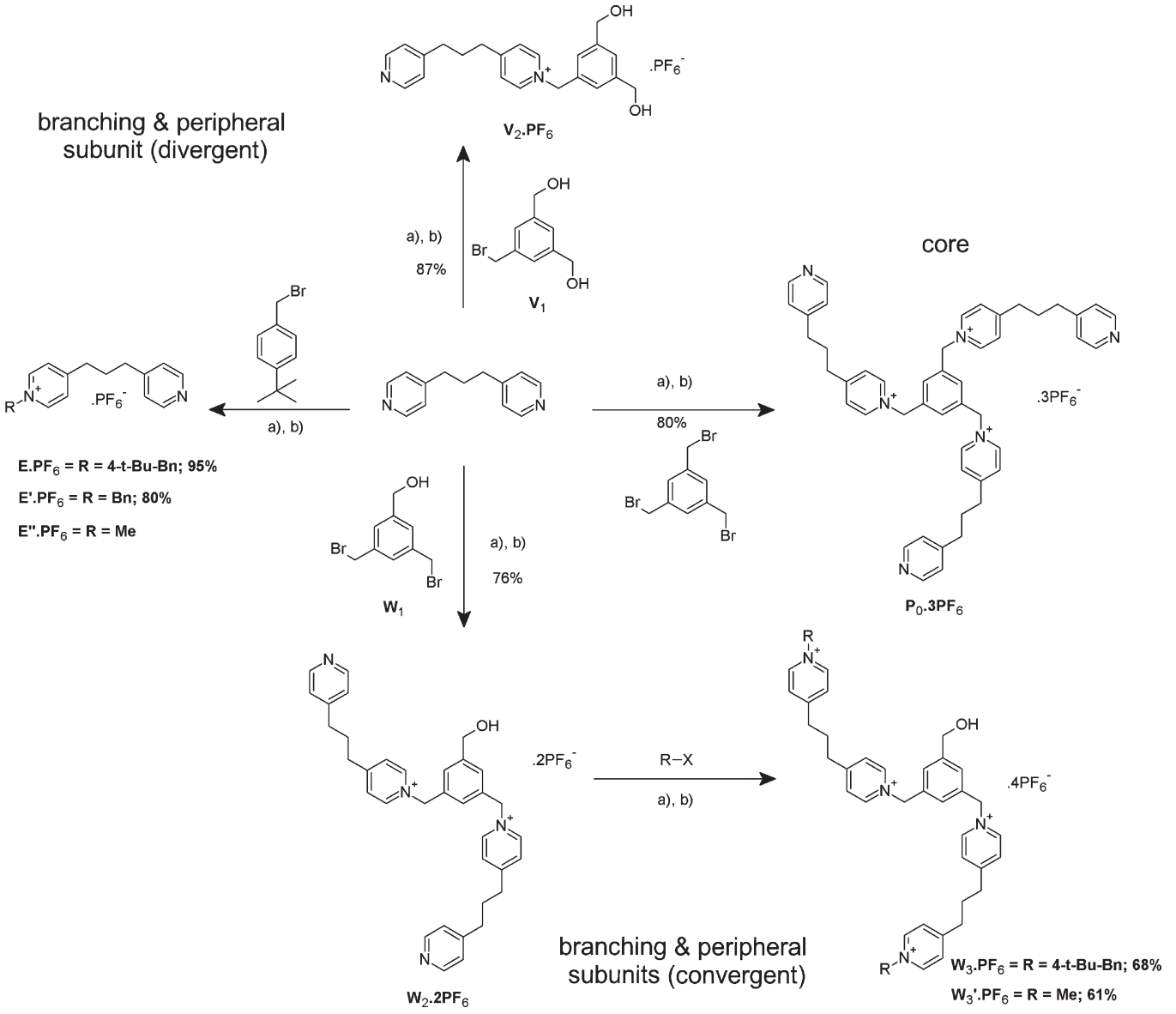

[a] Key: (a) CH_3CN/80 °C; (b) 3 M NH_4PF_6/H_2O.

unique or of general importance. Our new dendrimers exhibit cationic complexing functionalities distributed all through the core, the branches and the periphery. Di- and trianionic guests are efficiently complexed. For the first time we describe here evidence for an inside-out loading scenario that respects cationic dendrimer molecular shells similar to the Bohr atomic model.

Host−guest interaction studies were carried out on a model anticancer drug/DNA intercalator,[21] i.e. dianionic 2,6-anthraquinone disulfonate (AQDS). Notably, this guest is electroactive,[22] whereas the new dendrimers consisting of pyridinium sites do not show electroactivity at potentials > −1 V. The interactions between AQDS and the dendrimers were monitored using ^{1}H NMR, DOSY, and cyclic voltammetry.

2. Results and Discussion

a. Synthesis. The syntheses of the core, the branching and the peripheral units for a new class of polycationic dendrimers are presented in Scheme 1. Commercially available 4,4′-trimethylenedipyridine can be easily monoalkylated by reacting it with substoichiometric amounts of alkylating agents. The syntheses of the core $\mathbf{P_0}\cdot 3PF_6$, the branching unit for divergent ($\mathbf{V_2}\cdot PF_6$) and for the convergent strategies ($\mathbf{W_2}\cdot 2PF_6$), as well as the corresponding peripheral units $\mathbf{E}\cdot PF_6$, $\mathbf{E'}\cdot PF_6$ and $\mathbf{E''}\cdot PF_6$,[23] $\mathbf{W_3}\cdot 4PF_6$ and $\mathbf{W_3'}\cdot 4PF_6$ are shown in Scheme 1. We have recently reported on the synthesis of the benzylic bromides $\mathbf{V_1}$ and $\mathbf{W_1}$,[24] here they are reacted with 4,4′-trimethylenedipyridine to yield the branching units $\mathbf{V_2}\cdot PF_6$ and $\mathbf{W_2}\cdot 2PF_6$. The peripheral subunits carrying the 4-*t*-Bu−Bn ($\mathbf{E}\cdot PF_6$), benzyl ($\mathbf{E'}\cdot PF_6$), and Me ($\mathbf{E''}\cdot PF_6$) are easily available from the reaction of 4,4′-trimethylenedipyridine and substoichiometric amounts of 4-*t*-Bu−BnBr, BnBr, or MeI, respectively. The $\mathbf{W_3}$ type peripheral groups are available from the precursor $\mathbf{W_2}\cdot PF_6$ using the corresponding alkylating agents. Notably, $\mathbf{V_2}\cdot PF_6$, $\mathbf{W_2}\cdot 2PF_6$, and $\mathbf{W_3}\cdot 4PF_6$ carry latent functionality (benzylic −OH) which can be activated by bromination using HBr/HOAc. The salts obtained after each reaction are water/MeOH soluble bromides or mixed salts, for analysis and further reaction these products were converted to MeCN soluble PF_6^- salts; ion exchange was achieved by the precipitation of the bromide salts with 3 M NH_4PF_6 from water/MeOH. Notably, the ion exchange step is the major purification available in these syntheses.

Scheme 2. Synthesis of Poly(trimethylenedipyridinium) Dendrimers G_0 to G_2[a]

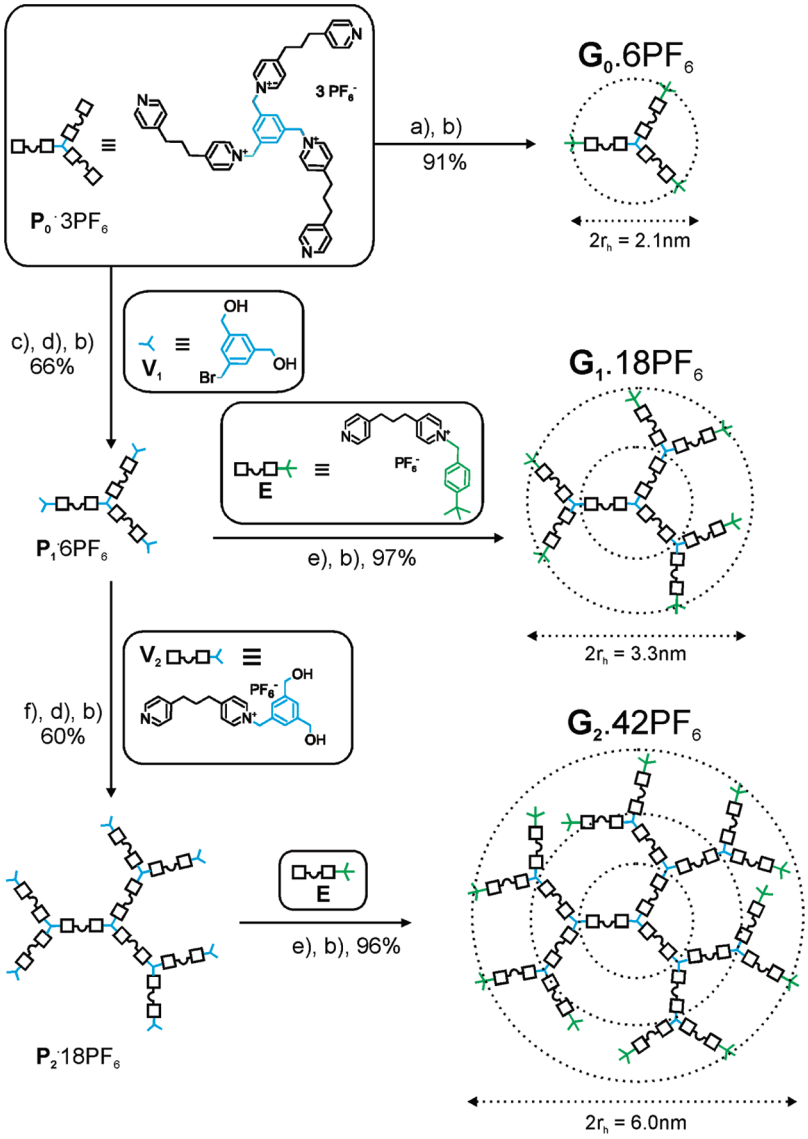

[a] Key: (a) 4-*t*-Bu−BnBr/CH_3CN/80 °C; (b) NH_4PF_6/H_2O; (c) $\mathbf{V_1}/CH_3CN$/80 °C; (d) HBr/HOAc/room temperature; (e) $\mathbf{E}/CH_3CN$/80 °C, (f) $\mathbf{V_2}/CH_3CN$/80 °C; yields reported are the isolated yields of the title compounds; dotted circles represent generation shells, r_h is the experimental hydrodynamic radius from DOSY.

The dendrimers of generations zero to two were synthesized following the "divergent method with preformed branching units"[15b] (Scheme 2). The three peripheral nitrogens in $\mathbf{P_0}\cdot 3PF_6$ react quantitatively with excess of benzyl bromide ($\mathbf{G_0}'$), methyl iodide ($\mathbf{G_0}''$) (not shown in Scheme 2, discussed in the Supporting Information) and 4-*t*-Bu−BnBr. The best yield and solubility were achieved with 4-*t*-Bu−BnBr as alkylating agent. Its reaction with $\mathbf{P_0}\cdot 3PF_6$ followed by ion exchange yielded $\mathbf{G_0}\cdot 6PF_6$ in 91%. For the synthesis of higher generations, the preformed branching unit, 3,5-bis(hydroxymethyl)-benzyl bromide ($\mathbf{V_1}$) was reacted with $\mathbf{P_0}\cdot 3PF_6$. The resulting hexol was activated by HBr/HOAc to give the hexabromide $\mathbf{P_1}\cdot 6PF_6$. [The crude hexol was first washed with CH_3CN to remove excess $\mathbf{V_1}$, and the resulting insoluble residue (mixed counterions) was directly brominated without further characterization. After bromination, $\mathbf{P_1}\cdot 6Br$ is obtained as a MeOH/H_2O soluble salt]. The branching unit $\mathbf{V_2}$ with one reactive pyridine nitrogen and two latent benzylic alcohol functionalities was used for the synthesis of the precursor $\mathbf{P_2}\cdot 18PF_6$. The yields of the precursors $\mathbf{P_1}$ and $\mathbf{P_2}$ were 66 and 60%, respectively, reflecting material loss in the ion exchange step. The dendrimers $\mathbf{G_1}\cdot 18PF_6$ and $\mathbf{G_2}\cdot 42PF_6$ were available from the reaction of the corresponding precursors $\mathbf{P_1}\cdot 6PF_6$ and $\mathbf{P_2}\cdot 18PF_6$ with the end group **E,** yielding 97 and 96%, respectively after ion exchange. The 4-*tert*-butylbenzyl groups impart better solubility, thus even dendrimers with mixed counterions are soluble in MeOH/H_2O and subsequent ion exchange gives MeCN soluble (MeOH/H_2O insoluble) PF_6 salts (for detailed synthetic procedures see Supporting Information).

The intermediates and products were characterized by ^1H NMR, ^{13}C NMR, and DEPT measurements. The purity of the compounds was further checked by elemental analysis (samples were pure apart from variable water contents) (see Supporting Information). The completeness of N-alkylation was generally followed based on the integration of the peripheral group as compared to the core resonances.

b. Host−Guest Complexation Studies. Host−guest complexation studies were carried out with $\mathbf{G_0}$, $\mathbf{G_1}$, and $\mathbf{G_2}$ dendrimers as host and anthraquinone-2,6-disulfonate (AQDS) as guest molecule. The molecular encapsulation of

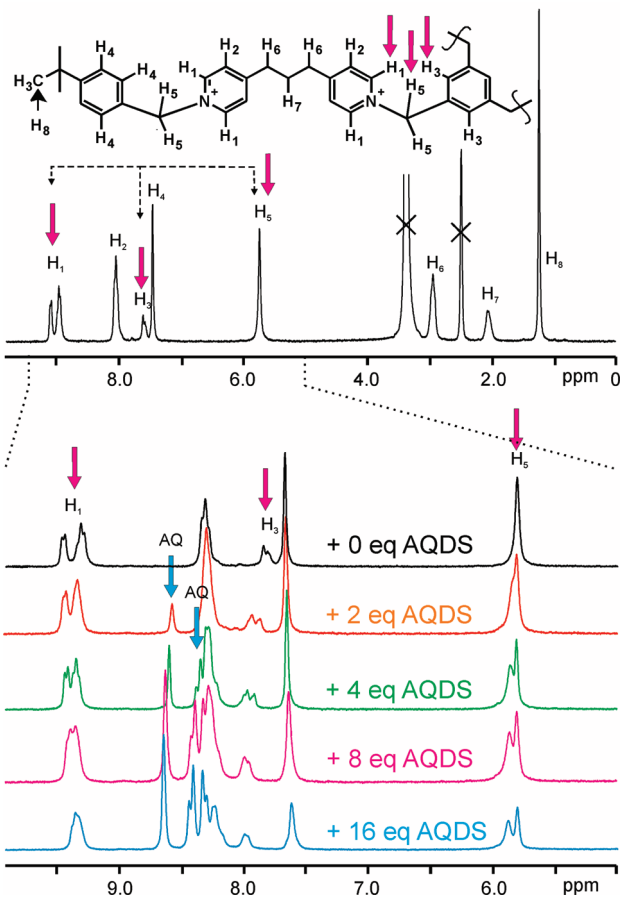

Figure 1. ^{1}H NMR spectrum of $\mathbf{G_1}$ (c = 2.8 mM in DMSO-d_6) with chemical shift assignment; magenta arrows: peaks monitored in guest titration (Figure 2); dotted-black arrows: resonances with cross peaks in NOESY (Supporting Information); AQDS equivalents present: black spectra, 0; orange, 2; green, 4; magenta, 8; blue, 16.

the dianion inside the dendritic voids is based on charge interactions and can be monitored using ^{1}H NMR techniques, DOSY, and cyclic voltammetry, as discussed below:

i. ^{1}H NMR Studies. ^{1}H NMR technique has been often used to evaluate the intermolecular interactions between host and guest in supramolecular chemistry. Complexation can show up (i) as cross-peaks in 2-dimensional NOESY between host and guest resonances as a function of complexation, or (ii) by a reduction of molecular symmetry and the splitting or variation in half-peak width of resonances from protons which become nonequivalent upon complexation.[25] Such host guest interaction on dendrimers monitored by NMR techniques have been reported by many research groups, e.g., by Astruc et al. (protonation of PAMAM dendrimers by different acids),[26] and Meijer et al. (hydrogen bonding interactions in adamantyl−urea functionalized PPI dendrimers).[8a,27]

Figure 1 shows the ^{1}H NMR of $\mathbf{G_1}$ including the complete assignment of the proton resonances. The corresponding spectra of $\mathbf{G_0}$ and $\mathbf{G_2}$ are similar except for the ratio of internal to peripheral protons (Supporting Information). The H_1 resonances on the pyridinium shows large splitting, whereas H_3 on the phenyl branching units show only minor splitting. This points to a preferential conformation of the methylene bearing H_5 rendering the two H_1—magnetically nonequivalent, but the three H_3—magnetically almost equivalent in the absence of the guest molecule (Supporting Information, Figure S3). Since the region from δ 0.9 to 4 (trimethylene and *t*-Bu end groups) is dominated by solvent peaks and tetrabutyl ammonium (counterion of the AQDS), we focused mainly on the changes in the region δ 5.7−9.1.

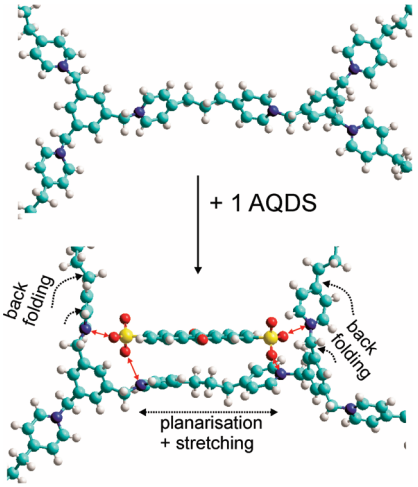

Figure 2. MM+ modeling of $\mathbf{G_1}$ before and after complexation of 1 AQDS. Black arrows indicate major changes in $\mathbf{G_1}$ conformation upon complexation; red arrows indicate electrostatic interactions.

The resonances due to meta-H_2 at pyridinium, as well as the protons at the trimethylene bridge (H_6 and H_7) show almost no splitting indicating reasonable rotational freedom of the bridge methylene groups (at least before complexation).

Upon addition of the dianionic guest AQDS, important shifts and changes in splitting of the host resonances H_1, H_3, and H_5 are observed as exemplified for the 18-fold positively charged $\mathbf{G_1}$ upon stepwise addition of 2, 4, 8, and 16 equiv of AQDS (1 equiv = 2 stoichiometric negative charges). The changes in chemical shift reach a constant value after complete charge compensation, i.e., 9 equiv of AQDS for $\mathbf{G_1}$. Interestingly, only intramolecular NOESY cross peaks are observed concerning the dendrimer protons H_1, H_3, and H_5 but not between dendrimer and aromatic protons of AQDS (Supporting Information).

The main conformational changes in the dendrimer upon complexation of a single AQDS have been modeled using the MM+ force field method (Figure 2). A good fit between the two sulfonates on a single AQDS and the two pyridinium nitrogens on a single propyl bispyridinium side chain is observed. Some stretching to an in-plane conformation of the propyl bridge and back-folding of the neighboring side chains is also typical.

A detailed study of the NMR shifts of the host protons H_1, H_3, and H_5 for all dendrimers $\mathbf{G_0}$−$\mathbf{G_2}$ as a function of added AQDS equivalents is shown in Figure 3. No precipitation is observed during the titration except for $\mathbf{G_2}$, for which the solution turned slightly hazy at the point of charge compensation. Generally changes become small above full charge compensation, but this is rather due to overcharging the dendrimer than to a low association constant (see later). Remarkably, prominent changes occur at the same number of added equivalents AQDS independent of the dendrimer generation, e.g. Three equiv of AQDS added leads to splitting of H_5 in $\mathbf{G_0}$, $\mathbf{G_1}$ and $\mathbf{G_2}$, or after 9 equiv of added collapse of the splitting of H_1 in $\mathbf{G_1}$ and $\mathbf{G_2}$ is observed. We interpret this behavior as follows (Figure 3, bottom):

The dendrimer $\mathbf{G_0}$ can be considered as a trimethylbenzene core with 3 doubly charged propyl bispyridinium side chains in a first shell, in $\mathbf{G_1}$, a further 2 × 3 = 6 doubly charged propyl bispyridinium side chains are added in a second shell,

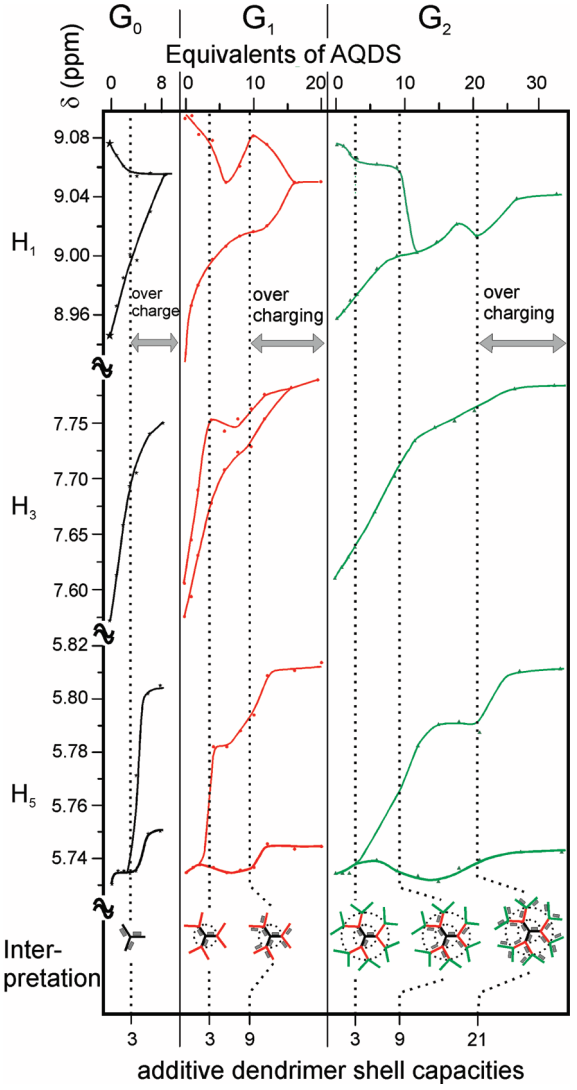

Figure 3. NMR titration: plots of the H_1, H_3, and H_5 dendrimer peaks of $\mathbf{G_0}$, $\mathbf{G_1}$, and $\mathbf{G_2}$ vs AQDS equivalent additions. [$\mathbf{G_0}$] = 6.9 mM; [$\mathbf{G_1}$] = 2.8 mM; [$\mathbf{G_2}$] = 1.1 mM. Dotted lines: dendrimer shell capacitance.

and in $\mathbf{G_2}$ another set of 4 × 3 = 12 doubly charged side chains are added in a third shell, yielding total amounts of 3, 3 + 6 = 9, and 3 + 6 + 12 = 21 doubly charged side chains organized in shells for $\mathbf{G_0}$, $\mathbf{G_1}$, and $\mathbf{G_2}$, respectively (Figure 3 (bottom), Scheme 2). The dotted lines connecting prominent changes in the splitting at 3, 9, and 21 equiv of AQDS are therefore evidence for a sequential filling of the innermost shell (3 open places), followed by the central shell (6 open places), followed by the outermost shell (12 open places). This conclusion is based on similar arguments as presented by Yamamoto et al. for phenylazomethine dendrimers complexing inorganic Lewis acids.[14f,20]

A similar study on the aromatic proton at δ 8.28−8.39 ppm of the guest molecule AQDS reveals a continuous, nonstructured shift of the resonance over a range of 0.1 ppm. Notably, the shift of free AQDS is reached at 30−100% excess of AQDS present in solution only. This points to overcharging the dendrimer at high AQDS concentration rather than incomplete complexation at the point of stoichiometric AQDS equivalents addition (Figure 4). The association constant for the first AQDS complexation by empty $\mathbf{G_2}$ ($K(\mathbf{G_2})$) can be estimated as $K(\mathbf{G_2}) > 1 \times 10^5$ from $c(\mathbf{G_2})_{\text{initial}}$ = 1.1 mM, $c(\text{AQDS})_{\text{initial}}$ = 1.1 mM, and $c(\mathbf{G_2}\text{-AQDS})/c(\mathbf{G_2})_{\text{initial}} > 0.9$.

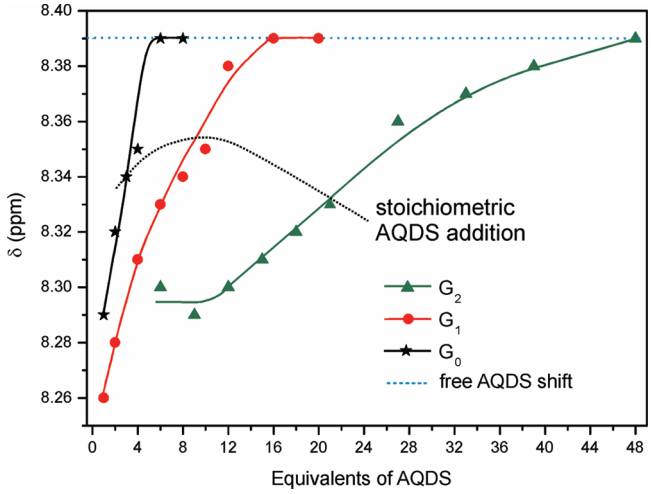

Figure 4. NMR titration: plots of the aromatic signal of AQDS at δ = 8.26 to 8.39. Key: dotted blue line, shift of the proton in the absence of a dendrimer; dotted black curve, connects stoichiometric equivalent additions for the three dendrimers.

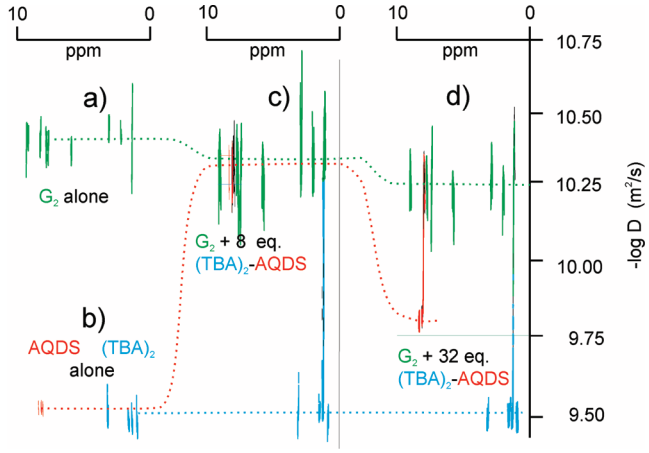

Figure 5. DOSY spectra: (a) $\mathbf{G_2}$ dendrimer; (b) AQDS$(TBA)_2$; (c) $\mathbf{G_2}$ dendrimer + 8 equiv of AQDS; (d) $\mathbf{G_2}$ dendrimer + 32 equiv of AQDS.

ii. Diffusion Ordered Spectroscopy. Diffusion ordered spectroscopy (DOSY),[28] recently emerged as an important technique in the study of host−guest complexes.[29] The prerequisite for such measurements is a sufficient difference in the diffusion coefficient of free host and free guest. Dendrimeric hosts fulfill this condition generally. DOSY has been successfully applied to probe the proton induced size variation of dendrimers terminated with $-NH_2$ or $-COOH$ groups.[30] Besides following the dendrimer diffusion coefficient, Astruc et al. found diffusion breakdown of the guest molecule upon complexation, e.g., interaction of acetylcholine with carboxyl-terminated dendrimers.[11a] Intermediate diffusion coefficient between complexed and free state has been explained for small guests by a fast bound-free ligand exchange mechanism.[11a] Besides complexation studies on a single dendrimer, DOSY can be used to study the dendrimer generation dependent diffusion coefficients.[9a,30] So far, very few DOSY studies are available on dendrimers size variation upon guest loading. The two most important concern (i) protonation-induced size change[30] and (ii) solvent-induced size change,[31] other studies show no or minor size changes upon guest complexation.[9b,11a]

The diffusion coefficients of the dendrimers $\mathbf{G_0}$, $\mathbf{G_1}$, and $\mathbf{G_2}$ were measured in DMSO-d_6. In the noncomplexed state each dendrimer displays relatively a narrow band of signals

Table 1. Diffusion Coefficients (D) and Hydrodynamic Radii (r_h) of Dendrimers in the Presence of Different AQDS Equivalent Additions (n)[a]

G_0			G_1			G_2		
n	$D \times 10^{-10}$ (m^2/s)[b]	$r_h \pm 0.05$ (nm)[c]	n	$D \times 10^{-10}$ (m^2/s)[b]	$r_h \pm 0.05$ (nm)[c]	n	$D \times 10^{-10}$ (m^2/s)[b]	$r_h \pm 0.05$ (nm)[c]
0	1.12	1.07	0	0.74	1.63	0	0.40	3.03
0.8	1.20	1.00	1	0.81	1.48	2	0.44	2.76
1.6	1.20	1.00	2	1.02	1.18	4	0.48	2.52
3.2	1.20	1.00	4	1.15	1.05	8	0.54	2.24
			8	1.26	0.96	16	0.60	2.00
			16	0.93	1.29	32	0.56	2.14

[a] $D_{AQDS} = 3.23 \times 10^{-10}$ m^2/s ($r_h = 0.37$ nm); $D_{TBA} = 3.46 \times 10^{-10}$ m^2/s ($r_h = 0.35$ nm); [G_0] = 6.7 mM; [G_1] = 2 mM; [G_2] = 0.97 mM. [b] Reproducibility and analysis error is ±5%.[36] [c] r_h is the hydrodynamic radius calculated for a hard sphere model.

centered at its average diffusion coefficient (ca. ± 20% in D maxima and minima with respect to the average). The trimethylene signals appear consistently at somewhat smaller D possibly due to overlapping with the solvent signals (Figure 5).[11b] The diffusion coefficients of G_0, G_1, and G_2 in the absence of AQDS are given in Table 1 (first line, $n = 0$). They cover a range of ca. 1.2 to 0.4×10^{-10} m^2/s corresponding to the hydrodynamic radii of 1.1 to 3.0 nm, respectively. In accordance, AQDS alone with its counterion tetrabutylammonium (TBA) displays $D_{AQDS} = 3.2 \times 10^{-10}$ m^2/s and $D_{TBA} = 3.5 \times 10^{-10}$ m^2/s (Figure 5b). (The hydrodynamic radii (r_h) were calculated using a hard sphere model with the Stokes−Einstein equation.

$$r_h = kT/6\pi\nu D$$

where k is the Boltzmann constant, $T =$ is the temperature in Kelvin, ν is the kinematic viscosity, $\nu = \mu/\rho$, μ is the viscosity,[32] ρ is the density of the solvent, and D is the diffusion coefficient.

Dendrimer generation dependent size studies have previously been reported.[9a,30] The more interesting results in the current stem from a study of the dendrimer DOSY spectra as a function of added guest molecules, i.e., equivalents of $AQDS(TBA)_2$ (Figures 5 and 6). In Figure 5c, we present G_2 in the presence of 8 equiv of $AQDS(TBA)_2$. The dendrimer shows a slightly faster diffusion coefficient than noncomplexed (dotted green line in Figure 5); the AQDS appears at the dendrimer diffusion coefficient (dotted red line, and its counterion remains at its original value clearly indicating complex formation). Upon further addition of $AQDS(TBA)_2$ equivalents—with equiv = 32 notably into the excess (overcharge) region—a further increase of the dendrimer diffusion coefficient is observed with the AQDS appearing in the dendrimer as well as at a diffusion coefficient intermediate between free $AQDS(TBA)_2$ and complexed, indicating fast exchange between the free and complexed state (Figure 5d).[9b,11a]

In Figure 6 and in Table 1, we resume the complete set of results on the diffusion coefficients of G_0, G_1, and G_2 as a function of AQDS added (in equivalents). Obviously all the polycationic host dendrimers shrink upon addition of the dianionic guest and reach the minimum size in the range of complete charge compensation. The shrinking concerns ca. 30% for G_1 and G_2, but it is only very small for G_0. Upon further addition of AQDS (overcharging), the dendrimers G_1 and G_2 grow again in size (Overcharging means that excess dianionic guests coordinate to the pyridinium subunits rendering the dendrimer all-over anionic. The repulsive interactions between the branches tend to expand the dendrimer structure). This is the first DOSY study that shows the mutual influence of complexation on host and guest diffusion coefficients in such an impressive manner. Probably it is related (i) to the fact that periphery and branches are carrier of fixed and persistent positive charge (endosystem in contrast to exosystem)[33] and (ii) to the fact that there exists a good fit of the two cationic sites on the propyl bispyridinium chain (preformed acceptor site) and the two sulfonate groups on the AQDS.

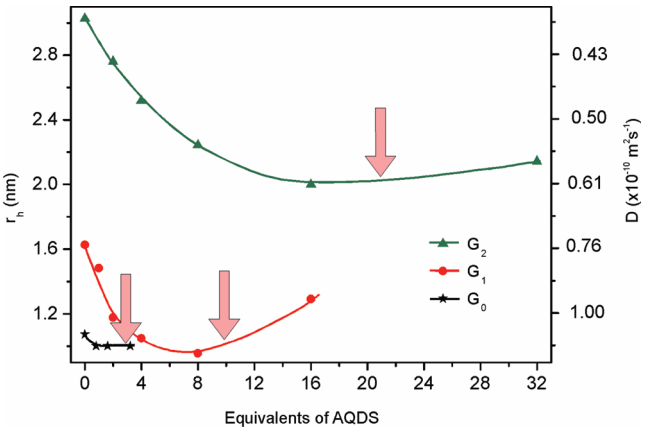

Figure 6. Diffusion coefficient (D) and hydrodynamic radii r_h as a function of the equivalents of AQDS, DOSY titrations. Pink arrows indicate formal charge compensation: [G_0] = 6.7 mM; [G_1] = 2 mM; [G_2] = 0.97 mM.

A lower limit for the association constant for the first AQDS complexation by empty G_2 ($K(G_2)$) can be estimated assuming more than 90% complexation (this is very conservative, as there is no indication of free AQDS even at 8 equiv addition!), thus yielding $K(G_2) > 1 \times 10^5$ (see Supporting Information).

iii. Cyclic Voltammetry. Cyclic voltammetry (CV) has been used in several cases to elucidate the interaction of redox-active guests with different supramolecular hosts. The CV curves deliver mechanistic, kinetic, and thermodynamic information about supramolecular host−guest interaction.[13a]

The dianionic AQDS alone shows two reversible reduction/oxidation waves on glassy carbon in DMF/0.1 M TBA·PF_6 with $E^{0\prime}_{1\_AQDS} = -0.826$ and $E^{0\prime}_{2\_AQDS} = -1.526$ (vs Ag/AgCl) according to

$$AQDS^{2-} + e^- \rightleftharpoons AQDS^{3-}$$

$$AQDS^{3-} + e^- \rightleftharpoons AQDS^{4-}$$

The dendrimers in the same solvent electrolyte system show two irreversible reductions with cathodic peak potentials in the range of −1.136 to −1.379 V depending on the generation and related to the reduction of the pyridinium moieties (Figure 7). A related modified electrode consisting of polypyrrole with pyridinium side chains and AQDS as a guest has earlier been reported.[22] However, this electrode was used in aqueous solution and AQDS under these conditions exhibits a two-electron−two-proton wave.

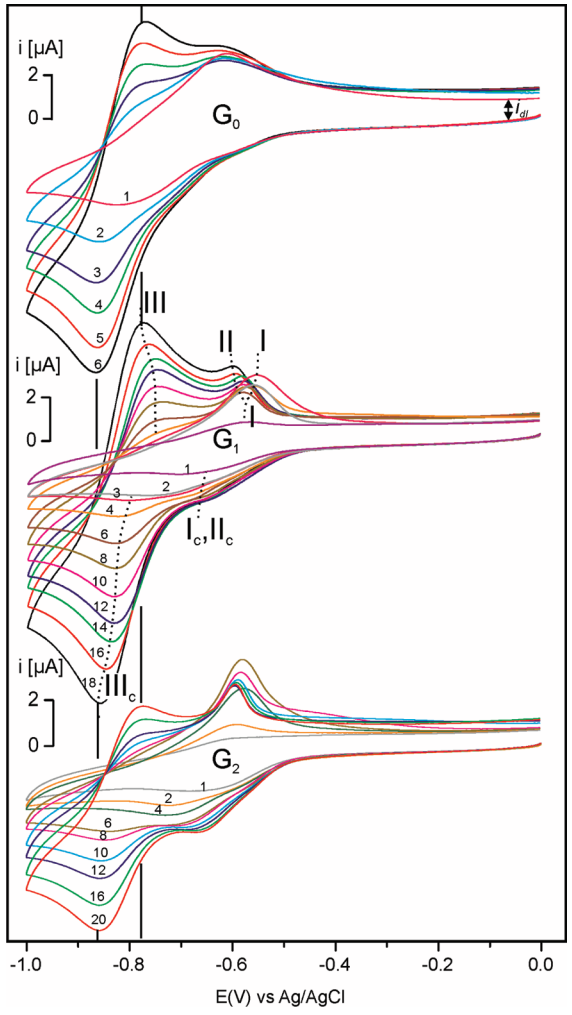

Figure 7. CV titration of $\mathbf{G_0}$, $\mathbf{G_1}$, and $\mathbf{G_2}$ dendrimer vs AQDS in DMF/0.1 M TBA·PF_6; $[\mathbf{G_0}]$ = 165 μM; $[\mathbf{G_1}]$ = 58 μM, and $[\mathbf{G_2}]$ = 35 μM. Numbers on each voltammogram indicate the number of added equivalents of AQDS.

In Figure 7, the cyclic voltammograms of $\mathbf{G_0}$, $\mathbf{G_1}$, and $\mathbf{G_2}$ in the presence of different equivalents of AQDS are presented (number of equivalents added are given in proximity of the corresponding CV). The scan was limited to the first reduction of AQDS, i.e. 0 to −1.0 V vs Ag/AgCl. The peak potentials of free AQDS (in the absence of dendrimers) are indicated by two vertical black lines. In the presence of dendrimers, the AQDS redox couple appears at more positive potentials. This is related to the preferential stabilization of the trianionic $AQDS^{3-}$ over the dianionic $AQDS^{2-}$ oxidation state by cationic dendrimer sites (Supporting Information, scheme of squares). For relative small equivalent additions, a small broad cathodic peak (I_c, II_c) and a larger symmetric anodic peak (I) is observed (as exemplified for $\mathbf{G_1}$ in Figure 7). The larger anodic and highly symmetric peak (I) is mainly due to adsorption of the complex upon reduction as confirmed by the electrode capacitance measurement (Figure 8). Upon further AQDS additions anodic peak II (diffusion controlled) develops, whereas the corresponding cathodic peak (I_c, II_c) becomes plateau shaped, accompanied by an increase in the electrode capacitance in the concentration range of total charge compensation. A new wave close to the potential of free AQDS develops for 4 and more equivalents as a reversible wave with E_{pc} III_c and E_{pa} III. A closer look reveals that—in spite of its proximity to the free AQDS

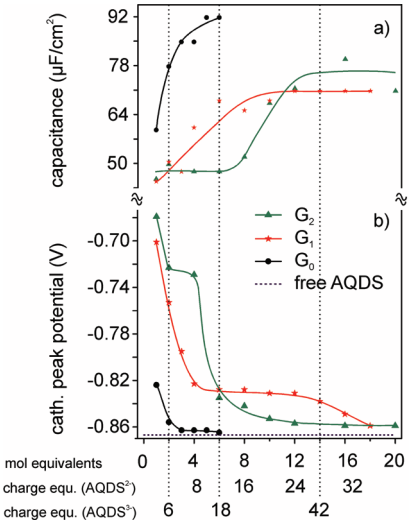

Figure 8. Plot of (a) the specific capacitance of the glassy carbon electrode at 0 V and (b) the cathode peak potential vs equivalents of AQDS as dianion or triple anion: $[\mathbf{G_0}]$ = 165 μM; $[\mathbf{G_1}]$ = 58 μM; $[\mathbf{G_2}]$ = 35 μM; specific capacitance of AQDS = 257 $\mu F/cm^2$; $\mathbf{G_0}$ = 207 $\mu F/cm^2$; $\mathbf{G_1}$ = 163 $\mu F/cm^2$; $\mathbf{G_2}$ = 157 $\mu F/cm^2$.

couple (black vertical lines)—AQDS is complexed by the dendrimer (see curved black dotted lines moving into the peak potentials of free AQDS for large guest concentration).

In parts a and b of Figure 8, the electrode capacitance and the reduction peak potential are plotted against AQDS equivalents. The capacitance curve shows prominent points at 6 equiv for $\mathbf{G_1}$ (corresponding to 9 equiv charge-corrected), 14 equiv for $\mathbf{G_2}$ (corresponding to 21 equiv if charge corrected). These points reflect a decrease of thickness of the adsorbate at the point of complete charge compensation influencing the pseudocapacitance, C_p with

$$C_p = (I_{dl}/\nu)$$

where I_{dl} is the double-layer capacitance (Figure 7), ν is the scan rate.[34]

From this equation, surface specific capacitance will be given by C_p/A, where A is the surface area of the working electrode.

A persistent adsorbat layer could explain the plateau character of peak I_c, II_c by the catalytic current related to the delivery of electrons through the adsorbate onto complexed dendrimers in solution. More important in the context of the description of the AQDS-dendrimer complex is the appearance of the shell capacity numbers (corrected for an additional charge because of the reduction), whatsoever, the correlation is less pronounced than in the NMR study.

iv. Modeling. Force field modeling MM+ implemented on Hyperchem 8.08[35] was used to judge the structure and size of the dendrimers as a function of the generation and upon guest complexation (Figure 9). Notably, these are gas phase calculation and therefore the charge interaction (each pyridinium carries +1, and each sulfonate oxygen −0.33) is severely overestimated. However, the general trends are in agreement with our experimental observations. $\mathbf{G_0}$ is almost flat except for the *tert*-butyl-benzyl end groups, whereas $\mathbf{G_1}$ and especially $\mathbf{G_2}$ show a dumbbell type ellipsoidal structure. Crude estimates of the large radii of the ellipsoids are given in Figure 9a. The ellipsoidal radii are 50−100% larger as compared to the hydrodynamic radii calculated from the diffusion coefficients (DOSY, Table 1) and a hard sphere model. However, all calculated structures are very "open"

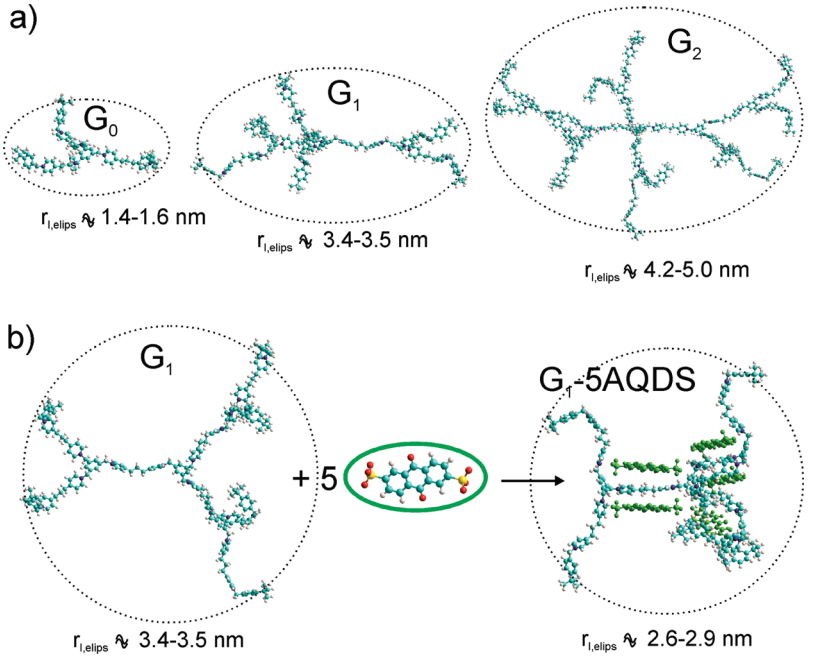

Figure 9. MM+ modeling of the dendrimers: (a) $\mathbf{G_0}$, $\mathbf{G_1}$, and $\mathbf{G_2}$ MM+ geometry optimized without counterions; unfavorable electrostatic interactions push the side chains at maximum distance from each other yielding dumbbell-type ellipsoidal structures for higher generations; presented ca. 70° out of the main ellipsoidal plane. (b) $\mathbf{G_1}$ relaxed as in part a but at 20° out of the main plane alone and after complexation of 5 molecules AQDS bearing one negative charge on each sulfonate. $R_{l,Ellips}$ = large radius of the ellipsoidal structures.

and allow much conformational freedom; definitely they are not hard spheres. Because of the unfavorable charge interaction the simulation drives the branches at maximum distance from each other. A limiting generation seems to be far away. Upon reaction with 5 equiv of AQDS, as exemplified for the case of $\mathbf{G_1}$ in Figure 9b, the arms fold back, the ellipsoidal radius decreases by ca. 20% ($r_{calc(free)}$ = 3.45, $r_{calc(5AQDS)}$ = 2.75) to be compared with the experiment showing a ca. 35% decrease ($r_{h(free)}$ = 1.63, $r_{h(5AQDS)}$ = ca. 1.02, Table 1). Other calculations also indicate severe contraction of the radii, if the dendrimer charge is counter balanced by anions carrying a single negative charge such as I^- or PF_6^- (Supporting Information).

3. Conclusions

In this work, we have introduced a new class of highly charged cationic dendrimers based on 1,3,5-tris-methylbenzene branching units interconnected by trimethylenedipyridinium. The synthetic strategy follows here a divergent approach but the intermediates necessary for a convergent route are also reported. The syntheses described are conceptually similar to the synthesis of the corresponding viologen dendrimers.[15b,24] In contrast to the viologen (4,4′-bipyridinium) dendrimers, the new trimethylendipyridinium dendrimers show no reversible electrochemistry (disruption of conjugation), they show higher flexibility (additional trimethylene), and they are expected to have a higher limiting generation (0.3 nm larger distance between the trimethylbenzene branching units). According to MM+ calculations (neglecting counterions and solvent) generation 0 has a disk conformation whereas generation 1 and 2 adopt open dumbbell type ellipsoidal conformations in order to minimize unfavorable charge interactions between the pyridinium moieties (Figure 9). The flexibility and the neglect of counterions account for a considerable overestimation of the corresponding theoretical hydrodynamic radii. In contrast, the use of a hard sphere model to calculate the hydrodynamic radius from the diffusion coefficient (from DOSY experiments) underestimates this parameter.

The model anticancer drug anthraquinone-2,6-disulfonic acid (AQDS)[21b] is a tailored guest for the new dendrimers. The two sets of negatively charged sulfonate oxygens (distance 1.1 nm) correspond well to the distance between the pyridinium nitrogens (distance 1.1 nm) in the trimethylenedipyridinium unit (Figure 2). Upon addition of substoichiometric amounts of the AQDS guest, the dendrimers contract and reach their smallest diameter (ca. 2/3 of their original hydrodynamic radius) in the range of total charge compensation (Figure 6). Overcharging with the AQDS guest is possible as evidenced by NMR (NMR titration, Figure 3) and cyclic voltammetry and leads to reopening of the dendrimer structure (increase of the hydrodynamic radius).

The dendrimers $\mathbf{G_0}$, $\mathbf{G_1}$, and $\mathbf{G_2}$ consist of 1, 2, and 3 concentric shells. The first shell can accommodate 6 counterions (3 equiv of AQDS), the second can accommodate 12 counterions (6 equiv of AQDS) and the third can host 24 counterions (12 equiv of AQDS). If charging occurs shell by shell we expect—in analogy to the Bohr atomic model—prominent changes in experimental observables for $\mathbf{G_2}$ at 3, 9, and 21 equiv AQDS added, if—and only if—the dendrimer is loaded "shell-wise" starting with the innermost shell. The appearance of such "magic numbers" was first and so far exclusively reported by Yamamoto et al for dendrimer-guest complexation based on Lewis base−Lewis acid interactions.[14f,20] We found—to the best of our knowledge for the first time for cationic dendrimers—clear evidence for a stepwise shell charging of the dendrimer from inside toward the periphery (Figure 3).

Preliminary experiments with other molecular guests and other cationic dendrimers point to the generality of the principle of stepwise guest filling in molecular shells. These further results are the subject of a forthcoming paper. We finally conclude from our results and from structural analogy that the trimethylene pyridinium dendrimers are appropriate transport vehicles for many negatively charged drugs (dianionic guests). Their expected low toxicity, and their high flexibility make them also suitable candidates for gene transfection.

Acknowledgment. M.K. thanks Graduate College 612 funded by the DFG for financial assistance. M. Gather's assistance during DOSY and NOESY measurements is greatly acknowledged.

Supporting Information Available: Text giving experimental details, detailed synthetic procedures, and calculation of association constants, figures showing spectroscopic and analytical data for new compounds, NOESY spectra, substructure from MM^+ simulation, scheme of squares, ^1H, ^{13}C, and DEPT spectra, and DOSY spectra, and two .mol files. This material is available free of charge via the Internet at http://pubs.acs.org.

References and Notes

(1) Buhleier, E.; Wehner, W.; Voegtle, F. *Synthesis* **1978**, 155.

(2) Tomalia, D. A.; Baker, H.; Dewald, J.; Hall, M.; Kallos, G.; Martin, S.; Roeck, J.; Ryder, J.; Smith, P. *Polym. J.* **1985**, *17*, 117.

(3) Newkome, G. R.; Yao, Z.; Baker, G. R.; Gupta, V. K. *J. Org. Chem.* **1985**, *50*, 2003.

(4) Hawker, C. J.; Frechet, J. M. J. *J. Am. Chem. Soc.* **1990**, *112*, 7638.

(5) (a) Carlmark, A.; Hawker, C.; Hult, A.; Malkoch, M. *Chem. Soc. Rev.* **2009**, *38*, 352. (b) Grayson, S. M.; Frechet, J. M. *J. Chem. Rev.* **2001**, *101*, 3819. (c) Mintzer, M. A.; Merkel, O. M.; Kissel, T.; Simanek, E. E. *New J. Chem.* **2009**, *33*, 1918. (d) Zeng, F.; Zimmerman, S. C.; Kolotuchin, S. V.; Reichert, D. E. C.; Ma, Y. *Tetrahedron* **2002**, *58*, 825. (e) Laufersweiler, M. J.; Rohde, J. M.; Chaumette, J.-L.; Sarazin, D.; Parquette, J. R. *J. Org. Chem.* **2001**, *66*, 6440. (f) Goh Sarah, L.; Francis Matthew, B.; Frechet Jean, M. J. *Chem. Commun.* **2002**, 2954. (g) Goodwin Andrew, P.; Lam Stephanie, S.; Frechet Jean, M. J. *J. Am. Chem. Soc.* **2007**, *129*, 6994. (h) Hourani, R.; Kakkar, A. *Macromol. Rapid Commun.* **2010**, *31*, 947.

(6) (a) Hecht, S. *J. Polym. Sci., Part A: Polym. Chem.* **2003**, *41*, 1047. (b) Nierengarten, J.-F. *Angew. Chem., Int. Ed.* **2005**, *44*, 2830. (c) Gitsov, I.; Lin, C. *Curr. Org. Chem.* **2005**, *9*, 1025.

(7) (a) Smith, D. K. *Adv. Mater.* **2006**, *18*, 2773. (b) Astruc, D.; Boisselier, E.; Ornelas, C. *Chem. Rev.* **2010**, *110*, 1857. (c) Lee, C. C.; MacKay, J. A.; Frechet, J. M. J.; Szoka, F. C. *Nat. Biotechnol.* **2005**, *23*, 1517. (d) Welsh, D. J.; Jones, S. P.; Smith, D. K. *Angew. Chem., Int. Ed.* **2009**, *48*, 4047. (e) Medina, S. H.; El-Sayed, M. E. H. *Chem. Rev.* **2009**, *109*, 3141. (f) Merkel, O. M.; Mintzer, M. A.; Sitterberg, J.; Bakowsky, U.; Simanek, E. E.; Kissel, T. *Bioconjugate Chem.* **2009**, *20*, 1799. (g) Schultz, L. G.; Zimmerman, S. C. *Pharm. News* **1999**, *6*, 25. (h) Mintzer, M.; Merkel, O. M.; Kissel, T.; Simanek, E. E. *PMSE Prepr.* **2008**, *99*, 132. (i) Smith, D. K. *Curr. Top. Med. Chem.* **2008**, *8*, 1187.

(8) (a) Pittelkow, M.; Christensen, J. B.; Meijer, E. W. *J. Polym. Sci., Part A: Polym. Chem.* **2004**, *42*, 3792. (b) Pittelkow, M.; Nielsen, C. B.; Broeren, M. A. C.; van Dongen, J. L. J.; van Genderen, M. H. P.; Meijer, E. W.; Christensen, J. B. *Chem.—Eur. J.* **2005**, *11*, 5126. (c) Hawker, C. J.; Wooley, K. L.; Frechet, J. M. J. *J. Chem. Soc., Perkin Trans. 1* **1993**, 1287. (d) Jansen, J. F. G. A.; de Brabander van den Berg, E. M. M.; Meijer, E. W. *Science* **1994**, *266*, 1226.

(9) (a) Boisselier, E.; Diallo, A. K.; Salmon, L.; Ornelas, C.; Ruiz, J.; Astruc, D. *J. Am. Chem. Soc.* **2010**, *132*, 2729. (b) Wu, Q.; Cheng, Y.; Hu, J.; Zhao, L.; Xu, T. *J. Phys. Chem. B* **2009**, *113*, 12934.

(10) Hofacker, A. L.; Parquette, J. R. *Angew. Chem., Int. Ed.* **2005**, *44*, 1053.

(11) (a) Boisselier, E.; Ornelas, C.; Pianet, I.; Aranzaes, J. R.; Astruc, D. *Chem.—Eur. J.* **2008**, *14*, 5577. (b) Therien-Aubin, H.; Zhu, X. X.; Moorefield, C. N.; Kotta, K.; Newkome, G. R. *Macromolecules* **2007**, *40*, 3644.

(12) Bard, A. J.; Faulkner, L. R., *Electrochemical Methods: Fundamentals and Applications*, 2nd ed., Wiley: New York, 2001.

(13) (a) Sobransingh, D.; Kaifer, A. E. *Langmuir* **2006**, *22*, 10540. (b) Kaifer, A. E. *Acc. Chem. Res.* **1999**, *32*, 62.

(14) (a) Pluth, M. D.; Raymond, K. N. *Chem. Soc. Rev.* **2007**, *36*, 161. (b) Kleppinger, R.; Mortensen, K.; Meijer, E. W. *PMSE Prepr.* **2002**, *86*, 139. (c) Aloshyna, M.; Medina, B. M.; Poulsen, L.; Moreau, J.; Beljonne, D.; Cornil, J.; Di Silvestro, G.; Cerminara, M.; Meinardi, F.; Tubino, R.; Detert, H.; Schrader, S.; Egelhaaf, H.-J.; Botta, C.; Gierschner, J. *Adv. Funct. Mater.* **2008**, *18*, 915. (d) Marchioni, F.; Venturi, M.; Credi, A.; Balzani, V.; Belohradsky, M.; Elizarov, A. M.; Tseng, H.-R.; Stoddart, J. F. *J. Am. Chem. Soc.* **2004**, *126*, 568. (e) Gitsov, I.; Lambrych, K. R.; Remnant, V. A.; Pracitto, R. *J. Polym. Sci., Part A: Polym. Chem.* **2000**, *38*, 2711. (f) Ochi, Y.; Fujii, A.; Nakajima, R.; Yamamoto, K. *Macromolecules* **2010**, *43*, 6570.

(15) (a) Heinen, S.; Meyer, W.; Walder, L. *J. Electroanal. Chem.* **2001**, *498*, 34. (b) Heinen, S.; Walder, L. *Angew. Chem., Int. Ed.* **2000**, *39*, 806. (c) Felderhoff, M.; Heinen, S.; Mulisho, N.; Websersinn, S.; Walder, L. *Helv. Chim. Acta* **2000**, *83*, 181.

(16) (a) Ronconi, C. M.; Stoddart, J. F.; Balzani, V.; Baroncini, M.; Ceroni, P.; Giansante, C.; Venturi, M. *Chem.—Eur. J.* **2008**, *14*, 8365. (b) Marchioni, F.; Venturi, M.; Ceroni, P.; Balzani, V.; Belohradsky, M.; Elizarov, A. M.; Tseng, H.-R.; Stoddart, J. F. *Chem.—Eur. J.* **2004**, *10*, 6361.

(17) (a) Asaftei, S.; De Clercq, E. *J. Med. Chem.* **2010**, *53*, 3480. (b) Bongard, D.; Bohr, W. (Germany). Application: DE DE, **2008**; 10 pp.

(18) (a) Bus, J. S.; Aust, S. D.; Gibson, J. E. *Environ. Health Perspect.* **1976**, *16*, 139. (b) O'Fallon, J. V.; Wright, R. W., Jr. *Anal. Biochem.* **1991**, *198*, 179. (c) Ross, J. H.; Krieger, R. I. *Drug Chem. Toxicol.* **1979**, *2*, 207. (d) Ross, J. H.; Lim, L. O.; Krieger, R. I. *Drug Chem. Toxicol.* **1979**, *2*, 193.

(19) McNerny, D. Q.; Leroueil, P. R.; Baker, J. R. *Wiley Interdiscip. Rev. Nanomed. Nanobiotechnol.* **2010**, *2*, 249.

(20) (a) Yamamoto, K.; Higuchi, M.; Shiki, S.; Tsuruta, M.; Chiba, H. *Nature* **2002**, *415*, 509. (b) Satoh, N.; Cho, J.-S.; Higuchi, M.; Yamamoto, K. *J. Am. Chem. Soc.* **2003**, *125*, 8104.

(21) (a) Wong, E. L. S.; Gooding, J. J. *Anal. Chem.* **2003**, *75*, 3845. (b) Zagotto, G.; Mitaritonna, G.; Sissi, C.; Palumbo, M. *Nucleosides Nucleotides* **1998**, *17*, 2135. (c) Batchelor-McAuley, C.; Li, Q.; Dapin, S. M.; Compton, R. G. *J. Phys. Chem. B* **2010**, *114*, 4094.

(22) Komura, T.; Mori, Y.; Yamaguti, T.; Takahasi, K. *Electrochim. Acta* **1997**, *42*, 985.

(23) Taffa, D. H.; Kathiresan, M.; Walder, L.; Seelandt, B.; Wark, M. *Phys. Chem. Chem. Phys.* **2010**, *12*, 1473.

(24) Kathiresan, M.; Walder, L.; Ye, F.; Reuter, H. *Tetrahedron Lett.* **2010**, *51*, 2188.

(25) Hu, J.; Cheng, Y.; Wu, Q.; Zhao, L.; Xu, T. *J. Phys. Chem. B* **2009**, *113*, 10650.

(26) Boisselier, E.; Liang, L.; Dalko-Csiba, M.; Ruiz, J.; Astruc, D. *Chem.—Eur. J.* **2010**, *16*, 6056.

(27) Boas, U.; Karlsson, A. J.; de Waal, B. F. M.; Meijer, E. W. *J. Org. Chem.* **2001**, *66*, 2136.

(28) (a) Morris, K. F.; Johnson, C. S., Jr. *J. Am. Chem. Soc.* **1992**, *114*, 3139. (b) Johnson, C. S., Jr. *Prog. Nucl. Magn. Reson. Spectrosc.* **1999**, *34*, 203. (c) Cohen, Y.; Avram, L.; Frish, L. *Angew. Chem., Int. Ed.* **2005**, *44*, 520. (d) Stejskal, E. O.; Tanner, J. E. *J. Chem. Phys.* **1965**, *42*, 288.

(29) (a) Pregosin, P. S.; Kumar, P. G. A.; Fernandez, I. *Chem. Rev.* **2005**, *105*, 2977. (b) Brand, T.; Cabrita, E. J.; Berger, S. *Prog. Nucl. Magn. Reson. Spectrosc.* **2005**, *46*, 159.

(30) Young, J. K.; Baker, G. R.; Newkome, G. R.; Morris, K. F.; Johnson, C. S., Jr. *Macromolecules* **1994**, *27*, 3464.

(31) Leclaire, J.; Coppel, Y.; Caminade, A.-M.; Majoral, J.-P. *J. Am. Chem. Soc.* **2004**, *126*, 2304.

(32) Kang, H.; Facchetti, A.; Jiang, H.; Cariati, E.; Righetto, S.; Ugo, R.; Zuccaccia, C.; Macchioni, A.; Stern, C. L.; Liu, Z.; Ho, S.-T.; Brown, E. C.; Ratner, M. A.; Marks, T. J. *J. Am. Chem. Soc.* **2007**, *129*, 3267.

(33) (a) Baars, M. W. P. L.; Meijer, E. W. *Top. Curr. Chem.* **2000**, *210*, 131. (b) Vogtle, F.; Gestermann, S.; Hesse, R.; Schwierz, H.; Windisch, B. *Prog. Polym. Sci.* **2000**, *25*, 987.

(34) Hoefer, M.; Bandaru, P. R. *Appl. Phys. Lett.* **2009**, *95*, 183108/1.

(35) HyperChem(TM) Professional 8.0.8, Hypercube, Inc.: Gainesville, FL.

(36) The diffusion coefficients reported are median values of the distribution. The error estimations reported in this work were the difference between maximum and minimum diffusion values.